Journal of Magnetic Resonance 308 (2019) 106596

Contents lists available at ScienceDirect

Journal of Magnetic Resonance

journal homepage: www.elsevier.com/locate/jmr

Machine learning in NQR TNT express detection system

Alexey Nevzorov *, Andrey Orlov, Dmitry Stankevich

Volgograd State University, Volgograd, Russia

ARTICLE INFO

Article history:
Received 29 April 2019
Revised 9 September 2019
Accepted 10 September 2019
Available online 13 September 2019

Keywords:
NQR signal of TNT
NQR signal detection
Machine learning in signal processing

ABSTRACT

Nuclear quadruple resonance (NQR) has excellent potential for the remote detection of nitrogen-containing substances, such as trinitrotoluene (TNT). However, using NQR techniques in security systems have some problems. For example, unknown temperature of the detecting explosives and low signal-to-noise ratio (SNR) leads to a priori uncertainty of the parameters of the NQR signal. In the article, we use machine learning methods for detecting the NQR signal. It allows us to increase speed and accuracy of TNT NQR signal detection. We have shown that proposed method of NQR signal detecting is more accurate and 100 times faster than alternative methods if temperature uncertainty is above 10 degrees. We achieve probability of NQR signal detection about 95% for SNR −15 dB.

1. Introduction

One of the promising methods for detection of nitrogen-containing explosives (such as TNT) is based on NQR spectroscopy [1]. It allows to remotely detect the explosive into closed bags, boxes etc. However, the methods based on the NQR have some problems. The main problem is extremely low NQR signal energy. It significantly decreases detection probability of signal due to the external interference in NQR band [2]. Frequently used method of signal detection in this case is method of a matching filtering. It allows detecting of the NQR signal in laboratory conditions, when all the parameters of a sample are known and controlled [3]. In real cases, such as detecting landmines or explosives in public areas, temperature and volume of samples are unknown. Works [4,5] show that value and history of temperature visibly change NQR spectrum. For example, the sample temperature is unknown in tens degrees range. In addition, the signal amplitude is proportional to the sample volume. It limits using of matching filtering.

There are some known methods for detection of signals with unknown parameters: energy detection method (ED) [6], a set of matched filters (SMF) [7], adaptive narrow-band filtering [8] and various methods of quasi-likelihood estimates [9]. Energy detection method is to estimation of signal energy in the signal frequency band. The method has low computational cost, but its true detection probability is low when the signal energy is unknown. External interference in the signal frequency band significantly decrease detection probability also. Main problem of SMF is to decreasing the detection probability with increasing ranges of parameter uncertainty. The maximum likelihood estimation methods are based on the solving of multidimensional optimization problem. Calculating of likelihood function for several thousand samples of the signal is difficult computation problem. Hence, it is significantly increase signal detection time. These methods of signal detection are not applicable in practice. It explains by rich spectral composition of NQR signal.

Besides these methods neural networks are used for detection [10,11] and classification [12,13] of weak and multifrequency signals. We propose to use machine learning methods for detecting signals used in NQR-based devices for detecting TNT. The neural network is trained on dataset, which consists of many cases of signals and noise parameters [14]. Using of machine learning allows keeping true detection probability of NQR signal with unknown parameters. Training requires large computational cost only one time, subsequently using of trained network is faster than quasi-likelihood methods.

2. Signal model

NQR detectors and spectrometers often use free induction decay signal method [15]. Model of this signal is exponentially damped sinusoids and additive noise:

$$y[n] = x[n] + \xi[n] = \sum_{k=0}^{K-1} A_k \sin(2\pi f_k n\Delta t + \varphi_k)\exp(-\gamma_k n\Delta t) + \xi[n]. \quad (1)$$

Here $n = 0, 1, 2, \ldots, N-1$, N is a number of signal samples ($N = 10^3$), K is the signal multiplicity, f_k is the frequency of the k-th sinusoid, $\gamma_k > 0$ is the decay coefficient, φ_k is the initial phase,

* Corresponding author.
E-mail address: terrapevt@mail.ru (A. Nevzorov).

https://doi.org/10.1016/j.jmr.2019.106596
1090-7807/

Table 1
Temperature dependences of spectral component frequencies of orthoclinic TNT NQR signal.

Sinusoid number, k	1	2	3	4	5	6
$f_k(T)$, kHz	0.12 T + 834	0.27 T + 784	0.2 T + 792	0.21 T + 783	0.14 T + 804	0.14 T + 798

Table 2
Parameters of the simulated TNT NQR signal and their uncertainty ranges.

Signal Parameter	Range of uncertainty
Temperature, K	253–323
Sinusoid amplitudes, A_k	0.16–1
Initial phase, φ_k	0–2π
SNR, dB	−30 to 0
γ_k, s^{-1}	$(0–5)\cdot 10^4$

A_k is the harmonic amplitude, $\xi[n]$ – normal white noise, Δt – sampling time (Δt = 0.1 μs). Usually in spectrometers real and imaginary part of the signal NQR is available. We analyze only real part of NQR signals, which is described by model (1).

We use model of the NQR signal of orthoclinic TNT in the 800–900 kHz frequency range with K = 6 obtained in real experiments. We take the values of parameters and uncertainty ranges as close as possible to real experimental data in the temperature range 253–323 K [4,5]. The temperature dependence of f_k is linear and well studied (see Table 1 [5]).

The parameter γ has nonlinear temperature dependence [4,16]. It was experimentally demonstrated that A_k substantially depends not only on the sample volume, but also on its temperature history [17]. Therefore, the coefficients A_k in model (1) are dimensionless and we chose it randomly and independently. Table 2 shows the values of the parameters and their uncertainty ranges for the TNT NQR signals modeled in accordance with model (1). SNR is determined by formula:

$$\mathrm{SNR} = 10\ \lg(E_s/E_n),$$

where E_s is the total signal energy and E_n is the noise energy. Typical form of simulated NQR signals is shown on Fig. 1. Here the amplitude is normalized to the maximum of the NQR signal.

3. Standard fast methods for detecting a TNT NQR signals

In the study, we compared three fast methods for detecting a TNT NQR signal: an energy detection method (ED), a method of matched filters set (SMF), and the proposed method that uses a neural network (NN).

The main ED method idea is comparing the signal energy E_s with the detection threshold. The signal $y[n]$ in filtered by the band-pass filter with cut-off frequencies of 830 and 900 kHz. The signal energy E_s is calculated from filtered signal samples $y'[n]$ by the formula:

$$E_S = \sum_{n=0}^{N-1} y'^2[n].$$

If $E_s > \delta$, then the signal is detected, otherwise not. The detection threshold δ is defined as:

$$\delta = \sum_{n=0}^{N-1} \left(\xi^2[n] + \frac{1}{2} x_{min}^2[n] \right),$$

where x_{min} is a signal with arbitrary frequencies, temperature and initial phases from Table 2 and minimal energy parameters (A_k = 0.16 and $\gamma = 5\cdot 10^4$).

SMF method was tested with N_{SMF} = 100 filters. The impulse responses of these filters h_j are the TNT $x[n]$ (1) NQR signals with

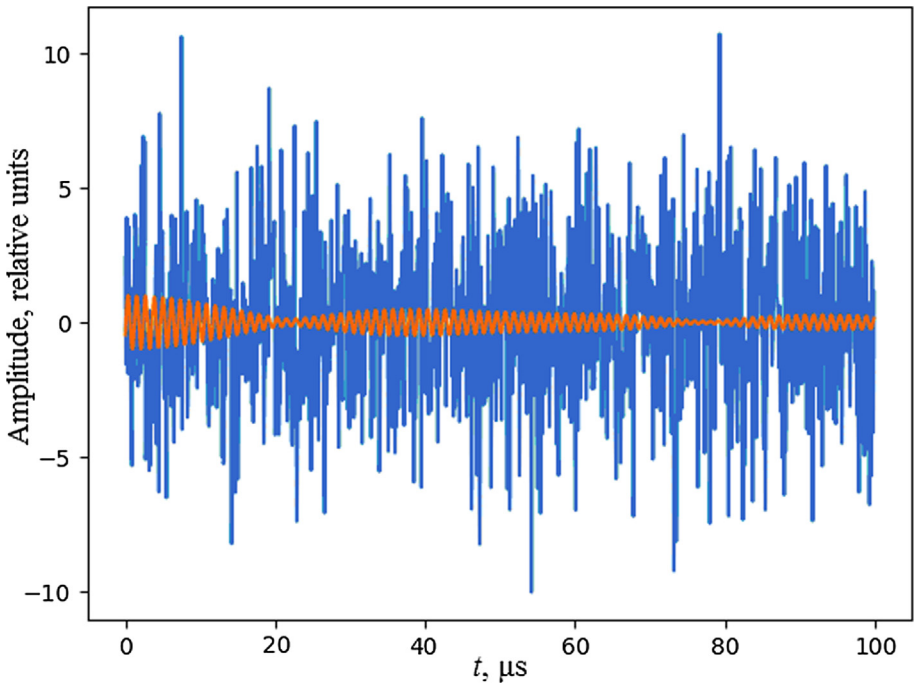

Fig. 1. TNT NQR signal with different SNR: −15 dB (blue) and without noise (orange). Signals are normalized to TNT NQR signal without noise. (For interpretation of the references to colour in this figure legend, the reader is referred to the web version of this article.)

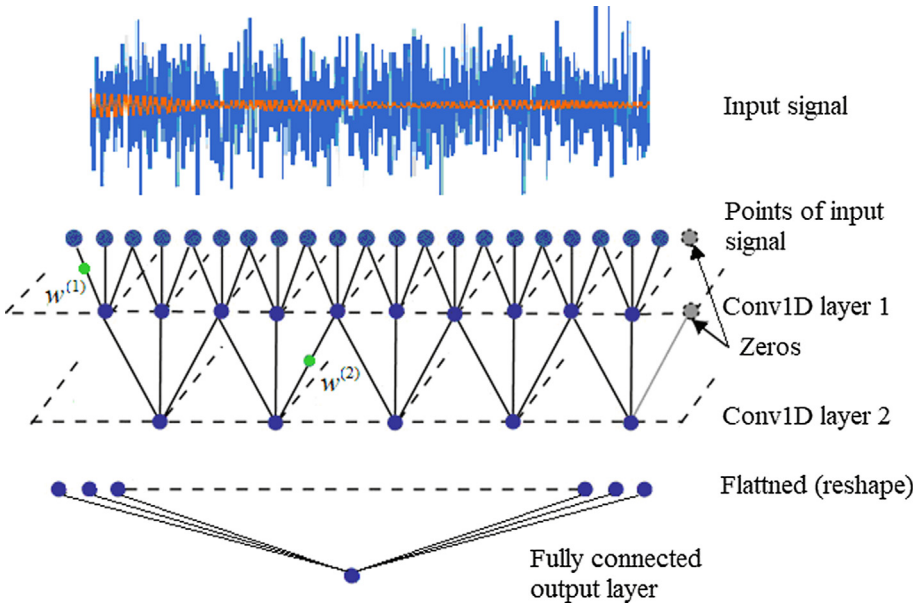

Fig. 2. Architecture of the neural network.

arbitrary parameters from Table 2. The analyzed signal $y[n]$ is processed by each of the created filters. The signal is detected with criterion of an ideal observer [18] if any inequalities are true:

$$\sum_{n=0}^{N-1} h_j[N-n-1]y[n] > \frac{1}{2}\sum_{n=0}^{N-1} h_j[N-n-1]h_j[n]. \quad (2)$$

4. The structure of the neural network and dataset

Two neural network's layers types are most often used for problems of detection and classification: fully connected and convolution layers [13]. We have found that the mixed architecture allows to achieve minimal true probability error with highest calculation speed. Proposed neural net consist of two one-dimensional convolution layers (Conv1D) and one fully connected layer. Our model of deep convolutional neural network is shown on Fig. 2. The net detail architecture is presented in Table 3. Main feature of convolutional network is large number of edges in computational graphs (about $1.2 \cdot 10^5$) but low count of neuron weights (3200).

Consider the signal transformation within the network layers. At first layer the signal $y[n]$ concatenates with L zeros before neural net processing. This procedure allows us to make all signals of a training set of same size ($N = 1000$). Adding zeros to the right or left does not matter. This is a standard procedure, described, for example, in [14]. The obtained signal $Y^{(0)}[n]$ transforms by the first convolution layer in following way:

$$z_r^{(1)}[n] = \mathrm{ReLU}\left(\sum_{l=0}^{L-1} w_r^{(1)}[l]Y^{(0)}[l+n] + b_r^{(1)}\right),$$

Table 3
Neural Network Architecture.

	Layer		
	1	2	3
Type	Conv1D	Conv1D	Fully connected
Neurons	10	20	1
Kernel, size × channels, stride	100 × 1, 1	10 × 10, 1	–
Max pooling, size, stride	10, 10	10, 10	–
Activation	ReLU	ReLU	Sigmoid

where L is the length of the convolution filters, $n = 0, 1,\ldots N-1$, $z_r^{(1)}[n]$ is the signal from the output of the first layer, $r = 0, 1,\ldots, R-1$, ($R = 10$ is the number of convolution filters), $w_i^{(1)}[l]$ is impulse responses of convolution filters, $b_r^{(1)}$ are the biases. The superscript in parentheses denotes the network layer number. The ReLU(x) function is defined as maximum between 0 and argument value x. The second layer input signals $Y_r^{(1)}[m]$ ($m = 0, 1,\ldots, N/S$, $S = 10$ is size of maximum pooling) are created from $z_r^{(1)}[n]$ by pooling operation [13] and L zeros padding.

$$z_r^{(2)}[m] = \mathrm{ReLU}\left(\sum_{l=0}^{L-1}\sum_{r'=0}^{R-1} w_{rr'}^{(2)}[l]Y_{r'}^{(1)}[l+m] + b_r^{(2)}\right),$$

where $w_{rr'}^{(2)}[m]$ are impulse responses of convolution filters in the second layer, $b_r^{(2)}$ are biases of the second layer filters. After the second convolution layer, pooling is performed again, to create 1-D flatten array $Y^{(2)}[q]$ ($q = 0, 1,\ldots, Q-1$, $Q = RN/S^2$ is the length of the flatten array $Y^{(2)}[q]$, from $z_r^{(2)}[m]$ for the third layer input. The last fully connected layer can be described by the formula:

$$\hat{p} = \left(1 + \exp\left(-b^{(3)} - \sum_{q=0}^{Q-1} w_q^{(3)}Y^{(2)}[q]\right)\right)^{-1},$$

here $\hat{p}$ is estimated quasi-probability of the NQR signal detection, $w_q^{(3)}$, $b^{(3)}$ are weights and biases of fully connected layer, respectively.

The weights, impulse responses and biases (w and b) of all layers are adjusted during the learning process. This process consists of minimizing the loss function, which in the case of a binary classification is average cross entropy for all dataset signals:

$$L(\theta) = -\frac{1}{M}\sum_{i-1}^{M}(p_i \log\hat{p}_i(\theta) + (1 + \mathrm{p_i})\log(1 - \hat{\mathrm{p}}_\mathrm{i}(\theta)))$$

Here M is the number of signals in the dataset, $\boldsymbol{\theta}$ is the parameters array (weights w and biases b) of the neural network, p_i is marker equal to "1" if signal consist TNT and "0" otherwise, $\hat{p}_i$ is the neural network's estimate of the probability of $x[n]$ being present on the y signal.

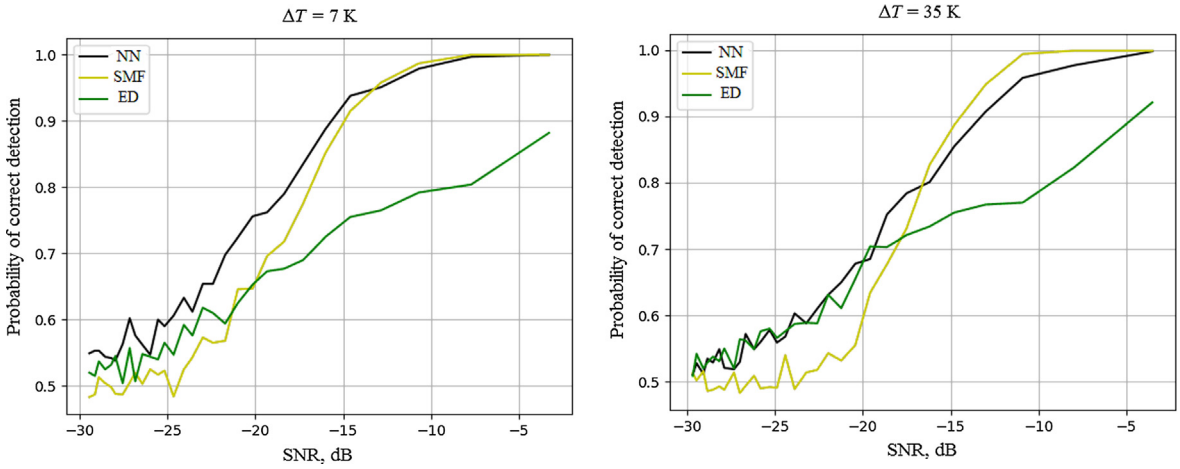

Fig. 3. Comparison of methods for two different ranges of temperature uncertainty ΔT: NN – black, SMF – yellow, ED – green lines. (For interpretation of the references to colour in this figure legend, the reader is referred to the web version of this article.)

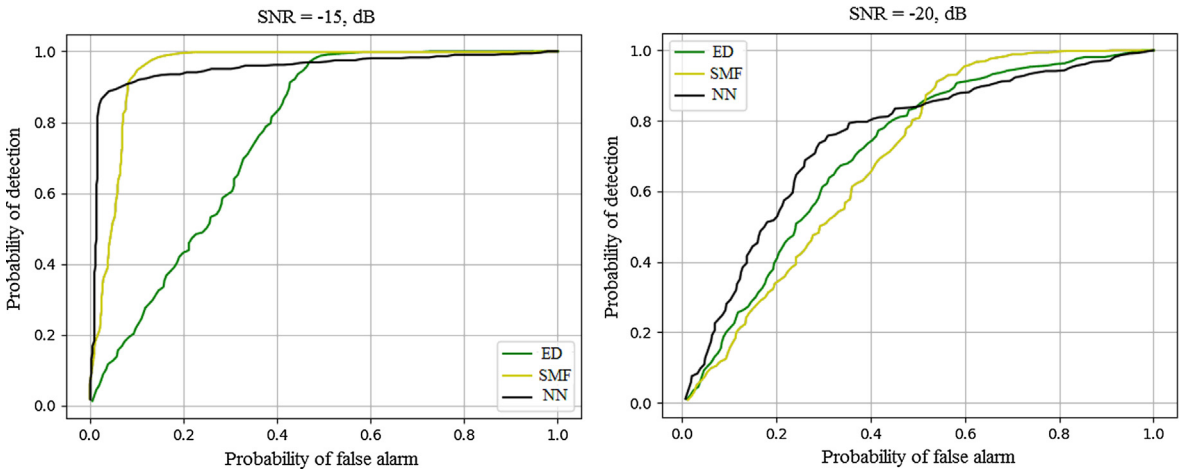

Fig. 4. ROC-curves for $\Delta T = 7$ K and different SNR: NN – black, SMF – yellow, ED – green lines. (For interpretation of the references to colour in this figure legend, the reader is referred to the web version of this article.)

Dataset consists of 2000 signals without NQR and 2000 TNT NQR model (1) signals (total count is $M = 4000$). Other model parameters are evenly distributed in the ranges defined by Table 2. Also the dataset is randomly divided into two equal size parts: training and test sets. The test set is used to calculate accuracy of trained neural network detector. A variation of the gradient descent method, the Adam method [19], is used to train the neural network. We use batches with 100 signals to accelerate training speed and to prevent overfitting of neural network model.

5. Experimental results

We compared the proposed method at different noise levels, for different ranges of temperature uncertainty of the TNT sample in three ranges 288 ± 0.5 K, 288 ± 7 K, 288 ± 35 K. In this case, the neural network in all experiments is trained in 253–323 K temperature range.

We study detection methods in SNR ranges from −30 dB to −5 dB. Low bound is defined as value then probability of correct detection is equal 0.5 for SMF. High bound is chosen as noise level when signal can be detected by spectrum maxima method. Dependencies of detection probability versus SNR for each method in two different ranges of temperature uncertainty are shown in Fig. 3. ED has low accuracy in any studied temperature range. Now we can see on Fig. 3 that NN is more accurately than ED if SNR > −20 dB but methods are same otherwise. SMF is more efficient than NN if SNR > −15 dB. NN is the best detection method if SNR < −10 dB and in lower temperature uncertainty case $\Delta T = 7$ K.

ROC-curves are used to estimate efficiency of detection methods [20]. ROC-curve is dependence probability of detection versus probability of false alarm. More effective detection method has larger area under curve. The ROC-curves for the studied methods for $\Delta T = 7$ K is shown on Fig. 4.

NN probability of detection is 85% with 1% probability of false alarm for SNR = −15 dB. SMF probability of detection is 35% for the same conditions, but areas under the ROC-curves are approximately equal. It means that efficiency of NN and SMF methods is equal if false alarm is not critical. All of these methods are not efficient for SNR < −20 dB. The methods are implemented on Python 3.5 and tested on i5 8600 CPU. Calculation times for each method are SMF – 0.35 s, ED – 0.01 s and NN – 0.015 s.

The python scripts that we used to calculate and implement the neural network detector are published in the github repository [21].

6. Conclusions

The method based on machine learning is more effective than alternative methods for detecting the TNT NQR signal with a large uncertainty of parameters. We achieved probability of NQR signal

detection about 95% for SNR −15 dB. Our investigation has shown that for our dataset, detection using neural networks is more effective for weaker signal, when the temperature of the substance is unknown. Neural network also minimizes interference error in task of NQR signal detection. We note that the described method does not require structural changes in the NQR detector equipment. Obviously, similar conclusions will be valid for the task of detecting the NQR signal of any substance. The neural network method of signals processing with uncertain parameters in strong noise can be used for signals of any kind, for example, spin echo signals. However, it should be noted that even in the described experiments, overfitting cannot be ruled out. Described approach can be improved in future research by optimization of training parameters and using robust dropouts or mixed pooling for overfitting cancellation.

Acknowledgements

The reported study was funded by RFBR and the government of Volgograd region according to the research project № 19-47-343004.

References

[1] Z. Bielecki, J. Janucki, A. Kawalec, J. Mikolajczyk, Sensors and systems for the detection of explosive devices – an overview, Metrol. Meas. Syst. 19 (2012) 3–28.
[2] H. Itozaki, G. Ota, Nuclear quadrupole resonance for explosive detection, Int. J. Smart Sens. Intell. Syst. 1 (2007) 705–715.
[3] A. Gregorovic, T. Apih, TNT detection with 14N NQR: multipulse sequences and matched filter, J. Magn. Reson. 198 (2009) 215–221.
[4] S. Somasundaram, A. Jakobsson, J. Smith, K. Althoefer, Exploiting spin echo decay in the detection of nuclear quadrupole resonance signals, Geosci. Remote Sens. IEEE Trans. 45 (2007) 925–933.
[5] J. Smith, J. Rayner, M. Rowe, J. Barras, Magnetic field-cycling NMR and 14N, 17O quadrupole resonance in the explosive pentaerythritol tetranitrate (PETN), J. Magn. Reson. 204 (2010) 139–144.
[6] 802.15.4a-2007, IEEE Standard for Information Technology — Telecommunications and Information Exchange Between systems — Local and metropolitan area networks — specific requirement. Parunt 15.4: Wireless Medium Access Control (MAC) and Physical Layer (PHY) Specifications for Low-Rate Wireless Personal Area Networks (WPANs), IEEE, N.Y., 2007. https://ieeexplore.ieee.org/servlet/opac?punumber=4299494.
[7] E. Beaucé, W. Frank, A. Romanenko, Fast Matched Filter (FMF): an efficient seismic matched-filter search for both CPU and GPU architectures, Seismol. Res. Lett. 89 (2017) 165–172.
[8] O. Hotra, A. Samila, L. Politansky, Synthesis of the configuration structure of digital receiver of NQR radiospectrometer, Przeglad Elektrotechniczny 1 (2018) 60–63.
[9] A.P. Trifonov, A.V. Kharin, Quasilikelihood estimate of the number of radio signals with unknown amplitudes and phases, Radiophys. Quant. Electron. 60 (2017) 159–170.
[10] S. Weihang et al., Detection of extremely weak NQR signals using stochastic resonance and neural network theories, Sign. Process. 142 (2018) 96–103.
[11] H. Gabbard, M. Williams, F. Hayes, C. Messenger, Matching matched filtering with deep networks for gravitational-wave astronomy, Phys. Rev. Lett. 120 (2017) 1–6.
[12] F. Amato, A. López, Artificial neural networks in medical diagnosis, J. Appl. Biomed. 11 (2013) 47–58.
[13] N.K. Ibrahim, R.S.A. Raja Abdullah, M.I. Saripan, Artificial neural network approach in radar target classification, J. Comput. Sci. 5 (2009) 23–32.
[14] S. Haykin, Neural Networks and Learning Machines, third ed., Pearson Education, 2009, p. 906.
[15] X. Zhang, N. Schemm, S. Balkır, M.W. Hoffman, A low-power compact NQR based explosive detection system, IEEE Sens. J. 14 (2014) 497–507.
[16] J. Smith, J. Rayner, M. Rowe, J. Barras, 14N NQR, relaxation and molecular dynamics of the explosive TNT, Solid State Nucl. Magn. Reson. 71 (2015) 61–66.
[17] R. Deas, K. Long, N. Peirson, An NQR study of the crystalline structure of TNT, Proc. SPIE – Int. Soc. Opt. Eng. 5415 (2004) 510–520.
[18] V.I. Tikhonov, Optimal Signals Reception, Radio and Connection Publ., Moscow, 1983, p. 320.
[19] D. Kingma, J. Ba, Adam: A Method for Stochastic Optimization, 2014, pp. 1–15. https://arxiv.org/pdf/1412.6980.pdf.
[20] T. Fawcett, An introduction to ROC analysis, Patt. Recogn. Lett. 27 (2006) 861–874.
[21] https://github.com/mrradist/nqr_detector repository.